Astron. Astrophys. 329, 986–990 (1998)

ASTRONOMY
AND
ASTROPHYSICS

High resolution spectroscopy of symbiotic stars⋆

III. Radial velocity curve for CD–43°14304

H.M. Schmid[1,2], **T. Dumm**[1], **U. Mürset**[1], **H. Nussbaumer**[1], **H. Schild**[1], **and W. Schmutz**[1]

[1] Institut für Astronomie, ETH-Zentrum, CH-8092 Zürich, Switzerland
[2] Landessternwarte Heidelberg-Königstuhl, D-69117 Heidelberg, Germany

Received 23 May 1997 / Accepted 17 July 1997

Abstract. We have obtained a series of high resolution optical spectra of the symbiotic system CD−43°14304. We derive the radial velocity curve of the cool component and determine an orbital period of about 1448 days and a mass function of m_f = 0.013 $M_\odot$ for this binary.

We present line profiles of Hα and the Raman scattered line at λ6825 for various orbital phases. The Hα line shows very strong variations in flux and spectroscopic structure which are locked to the orbital phase. Much less variability is seen in the Raman scattered line.

Key words: binaries: symbiotic — binaries: spectroscopic — stars: fundamental parameters — stars: individual: CD−43°14304

1. Introduction

Orbital parameters are fundamental for determining the stellar masses and the geometric configuration of binaries including symbiotic systems. Questions on the evolutionary status and on interaction processes can much better be addressed if the orbital parameters are well known.

This is the third paper in a series of publications (Schmutz et al. 1994; Schild et al. 1996) in which we determine orbital parameters of southern symbiotic systems from high resolution spectroscopy. Here we present new data on the high galactic latitude object CD−43°14304. The visual spectrum of CD−43°14304 shows the continuum absorptions of a cool giant with a spectral type of K5–M0 (Schulte-Ladbeck 1988) and strong emission lines of H I, He I, He II and the O VI Raman feature at λ6825 (Allen 1984). Far UV spectroscopy with IUE exhibits a very strong He II λ1640 line when compared to the emissions of C IV, N IV], N V, O III], and O IV] (Schmid & Nussbaumer 1993). CD−43°14304 shares this property with the well known population II symbiotic AG Dra. It may therefore be suspected that also CD−43°14304 is a metal poor system. For the white dwarf component a temperature of T^* = 110 000 K is estimated (Schmid & Nussbaumer 1993). Thanks to the low interstellar absorption, the hot component was also detected with ROSAT as a very soft X-ray source (Mürset et al. 1997).

In this paper we use high resolution spectroscopy to determine the radial velocity curve of the red giant in CD−43°14304. We obtain the orbital period and the mass function for this binary. We also present a series of line profiles of Hα and the Raman scattered O VI line at λ6825.

2. Observational data

In the course of a monitoring program of southern symbiotics, CD–43°14304 was observed with the Coudé échelle spectrograph (CES) fed by the 1.4 m Coudé auxiliary telescope (CAT) at La Silla (Table 1). The data were taken at a resolution of R = 60 000 and recorded with various CCDs. Most observations were carried out remotely from the ESO headquarters near Munich. We monitored the CD–43°14304 system with wavelength settings centred at 5007 Å, 6563 Å, 6830 Å, 7005 Å, 7450 Å, and 7505 Å. The wavelength coverage of an observation was ≈ 55 Å. Typical exposure times for one setting were about 20 − 60 min giving a typical signal to noise level between 20 and 40 in the continuum. Fig. 3 illustrates the quality of the obtained absorption spectra.

The data were reduced with the MIDAS software. The main steps were bias subtraction, flatfielding with a tungsten lamp spectrum, extraction, sky background subtraction (usually very low background) and wavelength calibration. The wavelength calibration is based on 15 – 20 lines of a thorium lamp. The individual arc lines agree to better than a 10th of a pixel or 0.25 km s^{-1} with the smooth dispersion curve. Radial velocities of CD−43°14304 determined within the same observing run (within a few days) agreed typically to about 0.7 km s^{-1}. This may be considered as a conservative estimate on the measuring

Send offprint requests to: H.M. Schmid, Heidelberg (hschmid@lsw.uni-heidelberg.de)

⋆ Based on observations obtained at the European Southern Observatory, La Silla, Chile

Table 1. Log of observations for CD−43°14304. The phase is calculated from the circular orbit solution given in Table 2. RV is the measured barycentric radial velocities of the cool giant and EW the emission line equivalent widths for Hα or the O VI Raman line λ6825.

JD (24...)	phase	λ central	RV [km s^{-1}]	EW [Å] Hα	EW [Å] λ6825
47256.84[a)]	0.917	6563	29.79	52	
47452.54[a)]	1.052	6563	32.30	69	
48405.78	1.710	6830	25.96		13.6
48509.75	1.782	6563	30.32	72	
48510.72	1.783	6830	29.38		10.4
48511.77	1.784	7005	28.98		
48551.57	1.811	6563	29.55	71	
48552.55	1.812	6830	28.58		8.9
48552.61	1.812	7005	28.52		
48698.91	1.913	6563	33.19	76	
48757.86	1.954	6563	33.90	105	
48758.88	1.954	6830	32.48		5.9
48831.87	2.005	7005	30.55		
48832.89	2.005	6830	30.54		7.7
48833.82	2.006	6563	31.03	130	
49131.85	2.212	6563	29.08	179	
49289.58	2.321	6563	26.53	215	
49290.56	2.322	7005	26.11		
49291.60	2.322	6830	25.32		10.7
49486.78	2.457	6563	23.88	119	
49523.91	2.483	7005	23.16		
49576.79	2.519	7505	26.05		
49657.58	2.575	7005	21.32		
49658.57	2.576	6563	21.75	104	
49857.92	2.713	6563	26.22	115	
49861.93	2.716	7450	25.19		
49974.66	2.794	7450	28.89		
50037.58	2.837	7005	30.51		
50038.57	2.838	6830	31.20		7.1:[b)]
50173.90	2.932	6563	33.33	135:[b)]	
50266.79	2.996	5007	29.56		
50283.79	3.007	5007	32.19		
50303.73	3.021	7005	31.91		

a) Observation from Van Winkel et al. (1993)
b) no early type star for continuum normalization

error as some short term radial velocity jitter may be intrinsic to the cool giant (see Sect. 3.1).

No absolute flux calibration was attempted, but a relative response was determined using observations of early type stars (except for JD 2450038 and JD 2450173). For the Hα setting, continuum points can be found only at the edges of the spectrogram.

3. The orbit of the cool giant

3.1. The radial velocity curve

As first step for determining the radial velocity of the cool giant we had to remove the nebular emission features. Therefore we clipped the strong Hα emission line in the λ6563 setting, and three weak lines due to O III], He I, and Fe II in the λ5007 setting. The Raman line in the λ6830 setting produces a relatively smooth bump (see Fig. 3), which was simply normalized in order to get an absorption spectrum with a continuum level of one.

Table 2. Orbital parameters of the cool giant. For the circular orbit (ε = 0) the entry T_0 gives the date of maximum radial velocity (RV-phase = 0), and for the eccentric orbit the date of periastron.

Parameter	circular	eccentric
P [d]	1448	1442
T_0 [JD]	2 445 929	2 445 560
V_0 [km s^{-1}]	27.6	27.5
K [km s^{-1}]	4.4	4.6
ε	0	0.22
ω	–	261°
$\sigma(O-C)$ [km s^{-1}]	1.28	1.14

Absolute radial velocities were determined by cross-correlating the individual observations of CD−43°14304 with spectra of the radial velocity standard stars α Hya (HR 3748, K3 II–III). We checked our radial velocities with additional measurements of the standard stars μ Psc (HR 434, K4 III) and α Cet (HR 911, M1.5 IIIa). The full widths at half maximum of the cross correlation peaks obtained are about $10-15$ km/s and the centre was determined by fitting a Gaussian to the peak.

In order to find the orbital parameters P, T_0, V_0, K, ε, and ω, we performed a least square fitting procedure. Table 2 gives the best solution for a circular orbit (ε = 0) and an eccentric orbit. The standard deviation $\sigma(O-C)$ of the observed values from the calculated fit is slightly smaller for the eccentric solution than for the circular solution. However, the $\sigma(O-C)$-values are still much larger than the estimated measuring error of $0.5-0.7$ km s^{-1}. We checked whether the residuals show some periodicity for example due to intrinsic pulsations. We found no obvious sign pointing to a non-random nature of the residuals. This points to the presence of short-term radial velocity variations (jitter) intrinsic to the cool giant. The same phenomenon is also seen in other symbiotic systems (see e.g. Smith et al. 1996) and luminous red giants (Jorissen & Mayor 1988). The jitter may perhaps be attributed to macroturbulence effects or low amplitude pulsations and seems to be related to the giant's luminosity. We refer the interested reader to the papers cited above for a more detailed discussion of this problem.

The presence of the radial velocity jitter introduces some uncertainty in the derived orbital parameters. We may estimate these uncertainties by varying the orbital parameters and comparing the fit solution with the data points. Inspection by eye suggest that fits with $\sigma(O-C) > 1.50$ km s^{-1} produce systematic deviations from the data points. Thus considering only fit solutions with $\sigma(O-C) \lesssim 1.5$ km s^{-1} we get the following uncertainty ranges for the parameters in Table 2: $\Delta P = \pm 100^{\rm d}$, $\Delta T_0 = \pm 300^{\rm d}$, $\Delta V_0 = \pm 0.7$ km s^{-1}, $\Delta K = \pm 1.0$ km s^{-1}, the upper limit $\varepsilon < 0.5$, and no constraints on ω. We emphasize

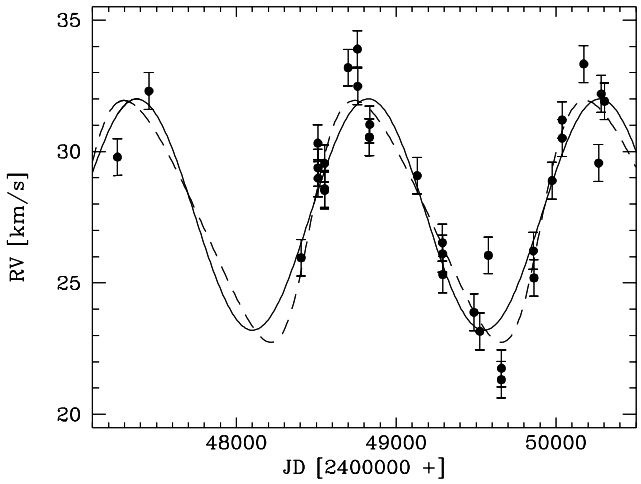

Fig. 1. Radial velocity curve for CD−43° 14304. The best circular orbit fit is given by a full curve and the best eccentric orbit fit by a dashed curve.

that the eccentricity obtained from the best fit solution (eccentric orbit) is not significant.

3.2. The mass function

With the parameters from the radial velocity curve we can derive the mass function $m_{\rm f}$ according to:

$$m_{\rm f} = \frac{1}{2\pi G} P K^3 (1-\varepsilon^2)^{3/2} = \frac{(M_{\rm h}\sin i)^3}{(M_{\rm h}+M_{\rm r})^2} \quad (1)$$

with $M_{\rm h}$ and $M_{\rm r}$ the masses of the hot and the cool component, i the orbit inclination, G the gravitational constant, P the period, and ε the eccentricity. Adopting the parameters from the circular orbit solution given in Table 2 yields

$$m_{\rm f} = 0.013\ {\rm M}_\odot\ . \quad (2)$$

The error range for $m_{\rm f}$ is rather large ($0.006\,{\rm M}_\odot$ − $0.025\,{\rm M}_\odot$). This reflects the uncertainty in the radial velocity semi-amplitude K introduced by the (intrinsic) jitter.

4. Line profiles

4.1. Hα

Fig. 2 shows the Hα line profiles as observed during about one orbital period from phase 1.78 to phase 2.71. There are remarkable differences in both, the line intensity, and spectral shape as function of orbital phase. Hα is strongest at around RV-phase 2.25, i.e. when the hot companion is in front of the red star. During this phase the line consists of a very strong main peak and a weaker blue component. During the observed period the blue component remained relatively unchanged while the main component showed strong and regular variations with phase. It changed from a minimum around $\phi \approx 1.75$ to a maximum at 2.25 and again a minimum around 2.75. Around "minimum"

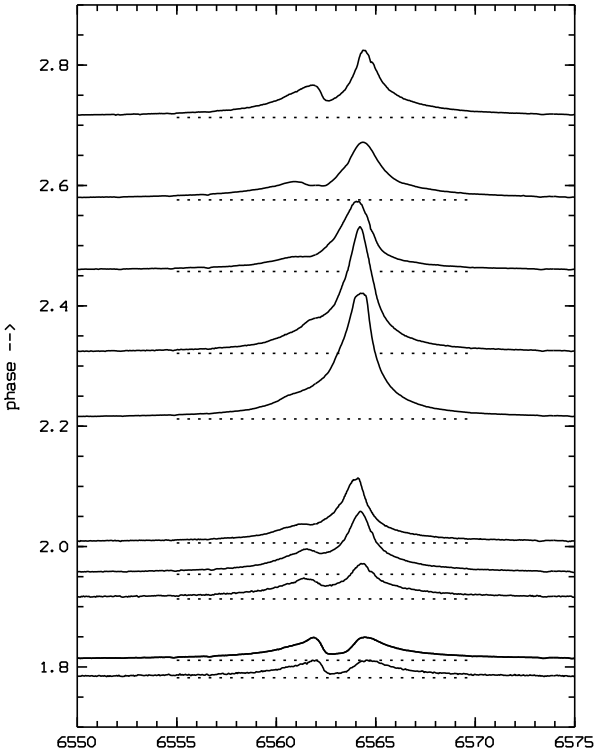

Fig. 2. Hα line profile evolution during one orbital period.

the blue and red component are about equal in strength. Similar changes in the Hα-profile are known to occur in several symbiotic systems. For example the coincidence of Hα flux maxima and minima with conjunction phases and the occurrence of the largest profile changes in the (red) main component are also observed in the eclipsing systems SY Mus and RW Hya (Schmutz et al. 1994; Schild et al. 1996). The observed behaviour strongly suggests an occultation (optical depth) effect in the Hα line which depends on the actual orientation of the binary (see also Schwank et al. 1997).

4.2. Raman line

The broad line around λ6825 is formed by Raman scattering of O VI λ1032 photons at neutral hydrogen (Schmid 1989). In symbiotic binaries it is assumed that the O VI radiation is produced in the ionized region near the hot component and converted into Raman photons by H^0-atoms in the neutral atmosphere and wind of the cool component.

In contrast to Hα, the Raman line at λ6825 shows relatively little variation (Fig. 3). In all our observations the profile is asymmetric with a steeper increase on the red side. The equivalent width is lowest for quadrature phase ($\phi \approx 2.0$) and enhanced for both conjunction phases, when the hot component is behind ($\phi \approx 1.75$) and in front ($\phi \approx 2.25$) of the red giant.

The intensity of the Raman scattered line depends on the incident O VI radiation field and the density distribution of neutral hydrogen (see e.g. Schmid 1996; Harries & Howarth 1997).

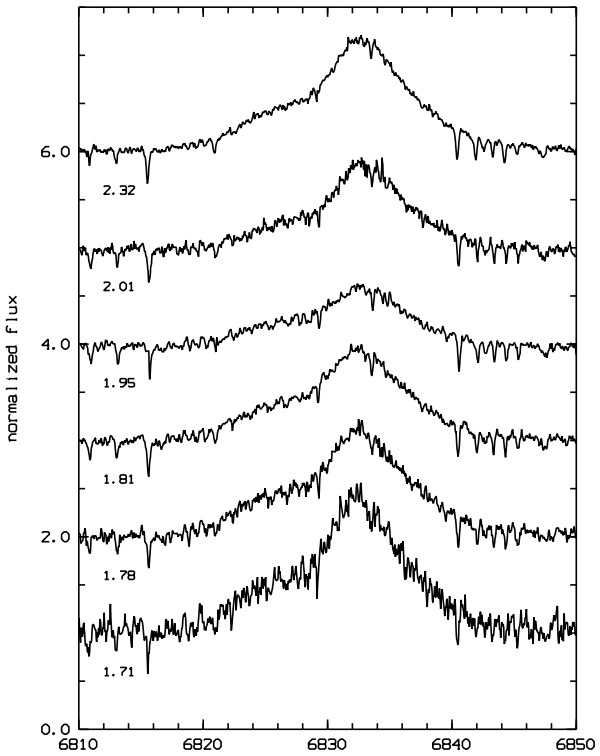

Fig. 3. Temporal variability of the Raman scattered O VI line at λ6825.

The observed flux variation of λ6825 resembles the model calculations XB3 in Schmid (1996). This suggests that the flux variations may be a result of the dipole-type scattering phase function of the Raman process. This phase function prefers forward and backward scattering and therefore conjunction phases when the O VI source and the scattering region are best aligned with the line of sight. The high intensity of the Raman line for the phase $\phi = 1.75$ (hot component behind the cool giant) indicates that the neutral scattering region is extended, so that only a small fraction can be occulted by the cool giant.

5. Rotation velocity of the red giant

The radial velocity curve of the M-star indicates an orbit with small or zero eccentricity. This implies that the rotation of the giant is probably synchronized with its orbital motion (Zahn 1977). We have compared the absorption line widths of the cool giant in CD$-43°14304$ with those of K3 III and M0 III stars. The comparison stars are believed to be single giants and have therefore a negligible rotation. The spectra used for the rotation analysis are centred at 7453 Å and have a resolution of $R = 100\,000$, they cover ~ 50 Å. We see no additional line broadening in CD$-43°14304$. This puts an upper limit on the projected rotational velocity of the red star of 3 km s^{-1}. As we have evidence for some occultation effects in the system, we assume that the orbital inclination is $i > 45°$. The red giant star radius then has to be smaller than $120\,R_\odot$.

6. Discussion

Good knowledge of orbital parameters is fundamental for our understanding of binary systems. In this paper we present radial velocity measurements for the cool giant of the symbiotic system CD$-43°14304$. We derive an orbital period of about 1450 days and a mass function of $m_f = 0.013\,M_\odot$. Thus we add another object to the relatively small list of symbiotic systems with radial velocity curves (see e.g. Garcia & Kenyon 1988; Mikolajewska 1997).

The accuracy of the derived mass function for CD$-43°14304$ is not good, due to the (intrinsic) radial velocity jitter. This phenomenon seems to be common in luminous red giants. Radial velocity studies of other symbiotics seem to suggest that this jitter is roughly random in nature (see e.g. Kenyon et al. 1991, 1993; Mikolajewska & Kenyon 1992; Mikolajewska et al. 1995; Smith et al. 1996). We may thus hope that more accurate mass functions may be gained by "simply" obtaining a larger data set.

CD$-43°14304$ shows a strong Raman line at λ6825 from which the orbit inclination may be determined polarimetrically as described in Schmid (1992, 1997) or Harries & Howarth (1996a). Existing spectropolarimetric observations (Schmid & Schild 1994; Harries & Howarth 1996b) show that the polarization angle in the Raman line does indeed rotate with time.

With the mass function and the inclination, we would be able to put stringent constraints on the masses of the stellar components. This is particularly interesting for CD$-43°14304$ as this object has in many respects properties very similar to the s-process element enriched object AG Dra (Smith et al. 1996). Better knowledge of such systems is important for understanding the evolutionary status of symbiotics, because s-process element anomalies in binary systems are often attributed to a Barium star like mass transfer scenario.

In addition we present a series of line profile observations of Hα and the Raman feature at λ6825 for CD$-43°14304$. Hα exhibits strong attenuation effects which are locked to the binary orbit. The Raman line shows smaller variations which may be attributed to the scattering phase function. Such time series of lines originating in different regions should help to clarify the geometric structure of the circumstellar material in the symbiotic system CD$-43°14304$.

Acknowledgements. We are indebted to the ESO staff at Garching and La Silla who, by their dedication, made the remote observations possible. We thank Steve Shore for clarifying discussions on the emission line variations. HMS acknowledges financial support by the Swiss National Science Foundation and the Deutsche Forschungsgemeinschaft (KR 1053/6-1).

References

Allen D.A., 1984, Proc. Astr. Soc. Austr. 5, 369
Garcia M.R., Kenyon S.C., 1988, in: The Symbiotic Phenomenon, IAU Coll. No. 103, J. Mikolajewska et al. (eds.), Kluwer, p. 27
Harries T.J., Howarth I.D., 1996a, A&A 310, 235
Harries T.J., Howarth I.D., 1996b, A&AS 119, 61
Harries T.J., Howarth I.D., 1997, A&AS 121, 15

Jorissen A., Mayor M., 1988, A&A 198, 187
Kenyon S.J., Oliversen N.A., Mikolajewska J., et al., 1991, AJ 101, 637
Kenyon S.J., Mikolajewska J., Mikolajewski M., Polidan R.S., Slovak M.H., 1993, AJ 106, 1573
Mikolajewska J., 1997, in: Physical Processes in Symbiotic Binaries and Related Systems, ed. J. Mikolajewska, Publ. Copernicus Found., Warsaw, p. 3
Mikolajewska J., Kenyon S.J., 1992, AJ 103, 579
Mikolajewska J., Kenyon S.J., Mikolajewski M., Garcia M.R., Polidan R.S., 1995, AJ 109, 1289
Mürset U., Wolff B., Jordan S., 1997, A&A 319, 201
Schild H., Mürset U., Schmutz W., 1996, A&A 306, 477
Schmid H.M., 1989, A&A 211, L31
Schmid H.M., 1992, A&A 254, 224
Schmid H.M., 1996, MNRAS 282, 511
Schmid H.M., 1997, in: Physical Processes in Symbiotic Binaries and Related Systems, ed. J. Mikolajewska, Publ. Copernicus Found., Warsaw, p. 21
Schmid H.M., Nussbaumer H., 1993, A&A 268, 159
Schmid H.M., Schild H., 1994 A&A 281, 145
Schmutz W., Schild H., Mürset U., Schmid H.M., 1994, A&A 288, 819
Schulte-Ladbeck R.E., 1988, A&A 189, 97
Schwank M., Schmutz W., Nussbaumer H., 1997, A&A 319, 166
Smith V.V., Cunha K., Jorissen A., Boffin H., 1996, A&A 315, 179
Van Winkel H., Duerbeck H.W., Schwarz H., 1993, A&AS 102, 401
Zahn J.P., 1977, A&A 57, 383

This article was processed by the author using Springer-Verlag LaTeX A&A style file *L-AA* version 3.